Femtosecond pulse with THz repetition frequency based on the coupling between quantum emitters and a plasmonic resonator

Shilei Li, Yinxing Ding, Rongzhen Jiao, Gaoyan Duan, and Li Yu[*]

State Key Laboratory of Information Photonics and Optical Communications, School of science, Beijing University of Posts and Telecommunications, Beijing 100876, China

Nanoscale pulsed light is highly desirable in nano-integrated optics. In this paper, we obtained femtosecond pulses with THz repetition frequency via the coupling between quantum emitters (QEs) and plasmonic resonators. Our structure consists of a V-groove (VG) plasmonic resonator and a nanowire embedded with two-level QEs. The influences of the incident light intensity and QE number density on the transmission response for this hybrid system are investigated through semiclassical theory and simulation. The results show that the transmission response can be modulated to the pulse form. And the repetition frequency and extinction ratio of the pulses can be controlled by the incident light intensity and QE number density. The reason is that the coupling causes the output power of nanowire to behave as an oscillating form, the oscillating output power in turn causes the field amplitude in the resonator to oscillate over time. A feedback system is formed between the plasmonic resonator and the QEs in the nanowire. This provides a method for generating narrow pulsed lasers with ultrahigh repetition frequencies in plasmonic systems using a continuous wave input, which has potential applications in generating optical clock signals at the nanoscale.

I. INTRODUCTION

In recent years, the coupling (both weak and strong) between quantum emitters (QEs) and plasmonic resonators has attracted much attention because of its various applications in quantum information [1,2], thresholdless lasing [3], and photon detectors [4]. We find that the coupling between QEs and plasmonic resonators can also be used to generate femtosecond pulses with ultrahigh repetition frequency in the case of a continuous wave input. Small on-chip pulsed lasers exhibiting mode sizes smaller than the emission wavelength represent an ideal solution for light source integration [5,6]. Plasmon pulsed lasers are especially promising for confining the emission below the diffraction limit while also exhibiting improved performance provided by enhanced emission dynamics [7–11]. Plasmonic waveguide-resonator (PWR) systems which guide radiation in the form of strongly confined surface plasmon-polariton modes represent a promising solution to manipulating light field at the nanoscale [12–18]. Fundamentally, strong localization of the field can enhance the energy exchange of QEs with light [19,20]. An attractive type of PWR is the V-groove (VG) waveguide-resonator system, which can strongly confine an electromagnetic field at the nanoscale and is promising for developing a planar plasmonic circuitry platform [21–25]. To the best of our knowledge, in the case of a continuous wave input, femtosecond pulses with THz repetition frequency are rarely reported in plasmonic resonator systems. Therefore, there is an increasing demand for femtosecond pulsed lasers with ultrahigh repetition frequency at the nanoscale.

In this paper, we investigate the influences of the incident light intensity and the QE number density on the transmission response for the hybrid system composed of a plasmonic VG resonator coupled to a nanowire embedded with QEs. In the weak-excitation limit, obvious mode splitting occurs in the transmission spectrum of the system, demonstrating that the coupling between the VG resonator and the QEs in a nanowire is remarkable. When the intensity of the excited light is strong, the population difference function $W(t)$ is no longer approximated as a constant, but as a function of time. The QEs in nanowire will oscillate between the upper and lower energy levels, thereby causing the output power of the nanowire to oscillate in pulse form, and then the transmittance of this system will also oscillate with time in pulse form. Moreover, it is found that the repetition frequency and extinction ratio of the pulses can be freely controlled by the incident light intensity and the QE number density. This provides a method for generating narrow pulsed lasers with ultrahigh repetition frequencies in plasmonic resonator systems.

II. STRUCTURE AND FIELD DISTRIBUTION

The structure shown in Fig. 1 consists of two plasmonic waveguides (S_1 and S_2), a VG cavity, and a nanowire embedded with QEs. The metal around the VG cavity is silver, the dielectric function of which is obtained from the experimental data of Johnson and Christy [26]. The transmittance of the system is numerically calculated using the finite difference time domain (FDTD) method. To excite the surface plasmon polaritons (SPPs), the input light is set to be a continuous wave (CW) of the transverse magnetic (TM) mode. The complex dielectric function of the nanowire embedded with QEs is described by a Lorentz model [27]: $\varepsilon(\omega) = \varepsilon_\infty - f\omega_L^2/(\omega^2 - \omega_L^2 + i\gamma\omega)$.
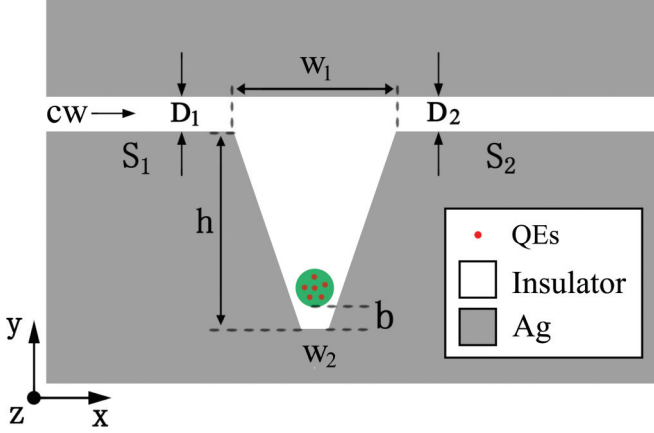
————————
[*]yuliyuli@bupt.edu.cn

FIG. 1. Schematic diagram of the hybrid system of a plasmonic VG resonator coupled to a nanowire embedded with QEs. The refractive index of the insulator is 1.41. The widths of waveguides S_1 and S_2 are respectively $D_1 = 30$ and $D_2 = 30$ nm. The width and height of the VG cavity are respectively $w_1 = 106$ nm and $h = 200$ nm, and the bottom width is $w_2 = 10$ nm. The diameter of the nanowire is 12 nm, and the distance from its bottom to the bottom of the VG cavity is $b = 5$ nm.

First, we investigate the distribution of the fields in a VG resonator without the nanowire. The distribution of the electric field $|E|$ on the dotted line q at different wavelengths is shown in Fig. 2(b). As can be seen from Fig. 2(b), the field enhancement in the VG cavity can reach maximum at the wavelength of 851 nm, and the electric field distribution is mainly concentrated near the bottom of the VG cavity. The distributions of the electric field components $|E_x|$ and $|E_y|$ at the resonant wavelength of 851 nm are respectively given in Figs. 2(c) and 2(d), from which it can be seen that the electric field component in the VG cavity is mainly $|E_x|$, and $|E_y|$ is almost zero. To obtain strong interaction between the electromagnetic fields and the emitters in nanowire, the nanowire should be placed near the bottom of the VG cavity,
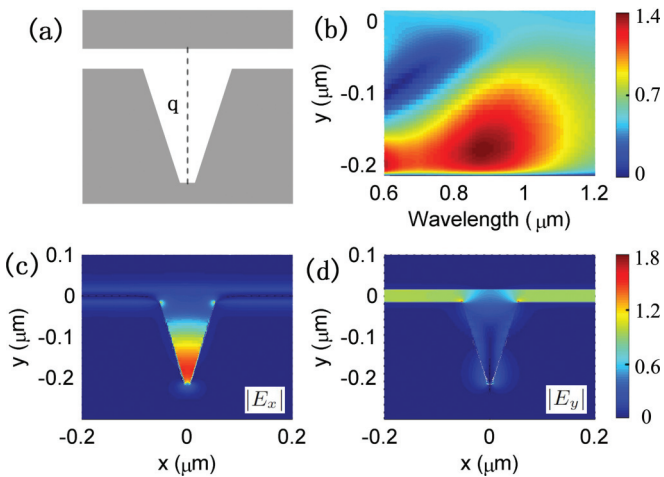

FIG. 2. (a) Schematic diagram and (b) distribution of electric field $|E|$ on the dotted line q at different wavelengths. (c) and (d) Distributions of the electric field components $|E_x|$ and $|E_y|$ at the resonant wavelength of 851 nm.

and the transition dipole moment of the QEs should be along the direction of the x axis.

Raza *et al.* investigated the optical response of the groove itself by electron energy-loss spectroscopy (EELS) [28]. The gap-surface-plasmon (GSP) modes can be classified according to the symmetry of the transversal electric component with respect to the mirror-symmetry plane of the groove (yz plane in Fig. 1). The symmetric GSP (sGSP) modes have an induced-charge pattern that is antisymmetric with respect to the mirror-symmetry plane, whereas the antisymmetric GSP (aGSP) modes are optically dark because of a symmetric induced charge distribution. And the results show that the excitation of the aGSP mode is related to the width of the groove. For widths $w_1 > 100$ nm, the aGSP mode is weakly excited because of the increased distance between the electron and the metal insulator interfaces. In the case of groove widths $w_1 < 100$ nm, the aGSP mode dominates the EELS data, which is signified by the strong dependence of the resonance peak on the groove width. Moreover, the aGSP mode absorption represents an additional (efficient) channel of energy dissipation that should be taken into account in the design of plasmonic resonator systems. In this paper, the parameter $1/\tau_{m0}$ in Eq. (5) in the next section is related to this energy dissipation.

III. WEAK-EXCITATION LIMIT

Next, we investigate the transmission response of this system in the weak-excitation limit. Based on the Bloch equation [29], the dipole transition equation for the interaction of the multimode electromagnetic field with the two-level system can be expressed as

$$\frac{d\rho_{eg}}{dt} = -(i\omega_A + \gamma)\rho_{eg} + iW(t)\sum_m \frac{g_m}{\sqrt{\varepsilon_0}E_{\text{vac}}^m}a_m \quad (1)$$

where ρ_{eg} is the dipole transition density matrix element, ω_A is the resonant frequency of the QEs in nanowire, γ is the decay rate, $W(t)$ is the population difference function, E_{vac}^m is the vacuum field of the mth mode, g_m is the coupling strength. According to the multimode interference coupled mode theory (MICMT) [30] and Heisenberg operator equations [31], it can be obtained that

$$\frac{da_m}{dt} = -\left(i\omega_m + \frac{1}{\tau_{m0}} + \frac{1}{\tau_{m1}} + \frac{1}{\tau_{m2}}\right)a_m$$
$$- ig_m\sqrt{\varepsilon_0}E_{\text{vac}}^m\rho_{eg} + \kappa_{m1}s_{m,1+} + \kappa_{m2}s_{m,2+}, \quad (2)$$

$$\kappa_{m1} = \sqrt{\frac{2}{\tau_{m1}}}, \quad \kappa_{m2} = \sqrt{\frac{2}{\tau_{m2}}}e^{-i\phi_m}, \quad (3)$$

$$s_{m,j+} = q_{mj}e^{i\varphi_{mj}}s_{j+}, \quad \sum_m q_{mj}e^{i\varphi_{mj}} = 1, \quad j = 1,2, \quad (4)$$

where a_m and ω_m are the normalized field amplitude and resonant frequency of the mth resonant mode, respectively. τ_{m0} is the decay time of the internal loss in resonator. τ_{m1} and τ_{m2} are the decay times of the coupling between the resonator and waveguides (S_1 and S_2), respectively. ϕ_m is the phase difference between the output port and input port of the mth resonant mode. s_{j+} are the field amplitudes in each waveguide. Here, we mainly consider the interaction
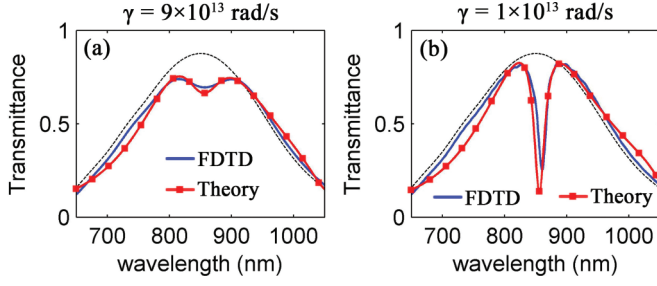
FIG. 3. The simulation results (blue lines) and theoretical results (red lines) for the transmittance of this hybrid system with the internal loss of the QEs are respectively (a) $\gamma = 9 \times 10^{13}$ rad/s and (b) $\gamma = 1 \times 10^{13}$ rad/s. The black dotted line is the simulation result of the transmittance of this system without nanowire. Here, the Lorentz model parameters of the nanowire are taken as $\varepsilon_\infty = 4.1, f = 0.4$ and $\omega_L = 2.17 \times 10^{15}$ rad/s. The fitting parameters are respectively $q_{k1} = 1, \varphi_k = 0, \omega_k = 2.17 \times 10^{15}$ rad/s, $\omega_A = \omega_k, \tau_k = 7$ fs, $\tau_{k0} = 48$ fs, $q_\delta = 0.3$, $\omega_\delta = 1.78 \times 10^{15}$ rad/s, $g_k = 7 \times 10^{13}$ rad/s, (a) $\varphi_\delta = 0.7\pi$, $\tau_\delta = 42$ fs, $\tau_{\delta0} = 40$ fs; (b) $\varphi_\delta = \pi$, $\tau_\delta = 150$ fs, $\tau_{\delta0} = 100$ fs.

between emitters and the kth mode whose resonant frequency is closest to the resonant frequency ω_A of the emitters, and ignore the interaction between the emitters and other modes whose resonance frequencies are far away from the resonant frequency of the emitters (that is, $g_m = 0$, $m \neq k$).

In the weak-excitation limit, the QEs are predominantly in the ground state, this means $W \approx -1$. If waveguides S$_1$ and S$_2$ are symmetric about the VG resonator, then $\tau_{m1} = \tau_{m2} = \tau_m$. And when $s_{2+} = 0$, the transmission coefficient of this hybrid system is

$$t = \frac{2q_{k1}e^{i\varphi_{k1}}(i\Delta_A + \gamma)}{\left(i\Delta_k\tau_k + 2 + \frac{\tau_k}{\tau_{k0}}\right)(i\Delta_A + \gamma) + \tau_k g_k^2}$$
$$+ \sum_{m \neq k} \frac{2q_{m1}e^{i\varphi_m}}{i(\omega_m - \omega) + 2 + \frac{\tau_m}{\tau_{m0}}}, \quad \varphi_m = \varphi_{m1} + \phi_m. \quad (5)$$

Then, the corresponding transmittance of this hybrid plasmonic system is $T = |t|^2$.

For ease of analysis, the overall effect ($\sum_{m \neq k} t_m$) of the mode whose resonant frequency is far from ω_A on the transmission response of this hybrid system is represented by a correction term $\delta = 2q_\delta e^{i\varphi_\delta}/[i(\omega_\delta - \omega) + 2 + \tau_\delta/\tau_{\delta0}]$. Thus, the transmission coefficient of this system is $t = t_k + \delta$. Simulation results (blue lines) and theoretical results (red lines) for the transmittance of this hybrid system with internal QE losses of $\gamma = 9 \times 10^{13}$ and $\gamma = 1 \times 10^{13}$ rad/s are given in Figs. 3(a) and 3(b), respectively. It is very difficult to theoretically provide some of the parameters (such as $\tau_k, \tau_{k0}, q, \varphi$, etc.) in Eq. (5) directly, because these parameters are related to the geometry of resonator, the width of waveguide, and the property of material. Therefore, some of the parameters in Eq. (5) need to be obtained by simulation and curve fitting. And the obtained parameters $\tau_k = 7$ fs and $\tau_{k0} = 48$ fs will be used in Sec. IV.

IV. NON-WEAK-EXCITATION LIMIT

The previous discussions were carried out under weak-excitation conditions. Obvious mode splitting occurs in the

transmission spectrum of this system, indicating that the coupling between the emitters and VG resonator is remarkable. When the excitation light intensity is sufficiently strong, the population difference function $W(t)$ is no longer approximated as a constant -1 in several cycles of the excitation light, but rather as a slowly varying function of time. This means that the output power of the nanowire is oscillatory. So, the transmission coefficient of the system will also oscillate over time. And the expression in Eq. (5) of the transmission coefficient is not applicable any more. Next, we will study the time evolution of the transmission coefficient when this hybrid system is at resonance.

According to the Bloch equation, the Bloch vectors (W, U, V) are

$$W = \rho_{ee} - \rho_{gg}, \quad U = \frac{1}{2}(\rho_{eg} + \rho_{ge}), \quad V = \frac{1}{2i}(\rho_{eg} - \rho_{ge}). \quad (6)$$

If the emitters (for which the internal loss is neglected) are in the ground state at the initial time, it can be obtained that

$$\frac{dW}{dt} = 2\Omega_R(t)[U \sin(\Delta_A t) - V \cos(\Delta_A t)], \quad (7)$$

$$\frac{dU}{dt} = -\frac{\Omega_R(t)}{2}W \sin(\Delta_A t), \quad (8)$$

$$\frac{dV}{dt} = \frac{\Omega_R(t)}{2}W \cos(\Delta_A t), \quad (9)$$

where $\Omega_R(t) = -\boldsymbol{\mu}_1 \cdot \boldsymbol{\psi}(\boldsymbol{r})|a(t)|/(\hbar\sqrt{\varepsilon_0}) = \chi|a|$, $\boldsymbol{\mu}_1$ is the transition dipole moment of one QE (take 0.5 nm in this paper), $\boldsymbol{\psi}(\boldsymbol{r})$ is the distribution function of the electric field (a) in VG cavity, ε_0 is the vacuum dielectric constant. When the system is at resonance ($\Delta_A = 0$), the above equation is simplified as

$$\frac{dW}{dt} = -2\Omega_R(t)V, \quad (10)$$

$$\frac{dV}{dt} = \frac{\Omega_R(t)}{2}W. \quad (11)$$

The initial condition is $W(0) = -1$, $\dot{W}(0) = 0$, $V(0) = 0$. Then, the solutions of Eqs. (10) and (11) are

$$W(t) = -\cos\left(\int_0^t \Omega_R \, dt\right), \quad (12)$$

$$V(t) = -\frac{1}{2}\sin\left(\int_0^t \Omega_R \, dt\right). \quad (13)$$

If the total number of QEs in nanowire is N and the mode volume of the resonator is V_{eff}, the number density of QEs in nanowire is $n = N/V_{\text{eff}}$. Ignoring the interaction between the QEs, the output power density of the nanowire is

$$p_{\text{nw}} = -n\hbar\omega_A \frac{1}{2}\frac{dW}{dt}$$
$$= -n\hbar\omega_A(\Omega_R/2)\sin\left(\int_0^t \Omega_R \, dt\right). \quad (14)$$

Equation (14) shows that the coupling between the electromagnetic field and the emitter causes the output power density of the nanowire to behave as an oscillating form. The oscillating output power in turn causes the field amplitude in the resonator

to oscillate over time. A feedback system is formed between the plasmonic resonator and the QEs in nanowire. We assume that a_{nw} is the extra field induced by the output power of the nanowire, a_0 is the field in plasmonic resonator without QEs in nanowire, a is the total field in the resonator. According to the coupled mode theory (CMT), the field in plasmonic resonator satisfies the following relationship:

$$\frac{da_0}{dt} = -\left(i\omega_k + \frac{1}{\tau_{k0}} + \frac{1}{\tau_{k1}} + \frac{1}{\tau_{k2}}\right)a_0 + \kappa_{k1}s_{1+} + \kappa_{k2}s_{2+},$$

(15)

$$s_{1-} = -s_{1+} + \kappa_{k1}^*(a_0 + a_{\mathrm{nw}}) = -s_{1+} + \kappa_{k1}^*a, \quad (16)$$

$$s_{2-} = -s_{2+} + \kappa_{k2}^*(a_0 + a_{\mathrm{nw}}) = -s_{2+} + \kappa_{k2}^*a. \quad (17)$$

For symmetric systems, $\tau_{k1} = \tau_{k2} = \tau_k$, and if $s_{2+} = 0$, then the solution of Eq. (15) is

$$a_0 = \frac{\kappa_{k1}s_{1+}}{i(\omega_k - \omega) + \frac{2}{\tau_k} + \frac{1}{\tau_{k0}}}, \quad (18)$$

and

$$s_{2-} = \kappa_{k2}^*a. \quad (19)$$

When the system is at resonance ($\omega_k - \omega = 0$), there is

$$\kappa_{k1}s_{1+} = \left(\frac{2}{\tau_k} + \frac{1}{\tau_{k0}}\right)a_0. \quad (20)$$

According to power conservation,

$$|s_{1-}|^2 + |s_{2-}|^2 = |s_{1+}|^2 + p_{\mathrm{nw}} - \frac{2}{\tau_{k0}}|a|^2, \quad (21)$$

and from Eqs. (16) and (19), it can be obtained that

$$2\left(\frac{2}{\tau_k} + \frac{1}{\tau_{k0}}\right)|a|^2 - \kappa_{k1}s_{1+}a^* - \kappa_{k1}^*s_{1+}^*a$$
$$= -\frac{\chi}{2}\sin\left(\int_0^t \Omega_R\,dt\right)n\hbar\omega_A|a|, \quad (22)$$

where $\chi = -\boldsymbol{\mu}_1 \cdot \boldsymbol{\psi}(\boldsymbol{r})/(\hbar\sqrt{\varepsilon_0})$. The excitation light in the waveguide is set as a simple harmonic wave $s_{1+} = |s_{1+}|e^{-i\omega t}$, then a_0 can be expressed as $a_0 = |a_0|e^{-i(\omega t + \theta)}$. Here, $|a_0| = |\kappa_{k1}s_{1+}|/|i(\omega_k - \omega) + 2/\tau_k + 1/\tau_{k0}|$ and $\theta = \arctan[(\omega_k - \omega)/(2/\tau_k + 1/\tau_{k0})]$. Since the quantum states of stimulated radiation and excitation light are the same, $a_{\mathrm{nw}} = |a_{\mathrm{nw}}|e^{-i(\omega t + \theta)}$ and $a = (|a_0| + |a_{\mathrm{nw}}|)e^{-i(\omega t + \theta)}$. When the system is at resonance, based on Eq. (20), we can obtain that

$$\kappa_{k1}s_{1+}a^* = \left(\frac{2}{\tau_k} + \frac{1}{\tau_{k0}}\right)a_0a^* = \left(\frac{2}{\tau_k} + \frac{1}{\tau_{k0}}\right)|a_0||a|, \quad (23)$$

$$\kappa_{k1}^*s_{1+}^*a = \left(\frac{2}{\tau_k} + \frac{1}{\tau_{k0}}\right)a_0^*a = \left(\frac{2}{\tau_k} + \frac{1}{\tau_{k0}}\right)|a_0||a|. \quad (24)$$

Therefore, both $(\kappa_{k1}s_{1+}a^*)$ and $(\kappa_{k1}^*s_{1+}^*a)$ are real numbers, then Eq. (22) is simplified as

$$\left(1 + \frac{\tau_k}{2\tau_{k0}}\right)(|a| - |a_0|) + \frac{\chi\tau_k}{8}\sin\left(\int_0^t \Omega_R\,dt\right)n\hbar\omega_A = 0. \quad (25)$$
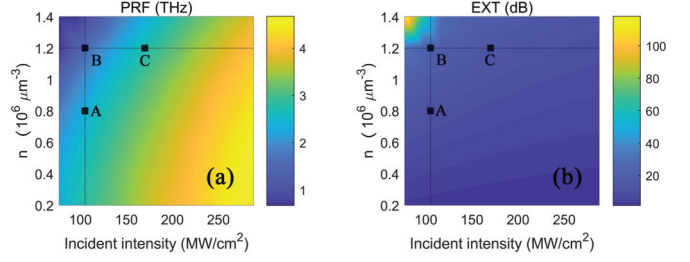

FIG. 4. Color-coded graphs for the influence of the incident intensity and QE number density on the repetition frequency and the extinction ratio of the pulses. The incident light intensity is expressed as $I_{\mathrm{in}} = c|a_0|^2/(n_{\mathrm{eff}}T_0)$, c is the speed of light in free space, $n_{\mathrm{eff}} = 1.62$ is the effective refractive index of the waveguide, and $T_0 = 0.87$. The nanowire is placed at the position of $\boldsymbol{\psi}(\boldsymbol{r}) = 1$.

The transmittance of the system is

$$T = \left|\frac{s_{2-}}{s_{1+}}\right|^2 = \left|\frac{2}{i(\omega_k - \omega)\tau_k + 2 + \frac{\tau_k}{\tau_{k0}}}\right|^2 \left|\frac{a}{a_0}\right|^2$$
$$= T_0\left|\frac{a}{a_0}\right|^2. \quad (26)$$

T_0 is the transmittance of the system when there is no QE in nanowire. The oscillating field amplitude (a) can be obtained from Eq. (25). And Eq. (26) shows that the oscillating field amplitude causes the transmittance of the system to oscillate over time. Based on Eqs. (25) and (26), we will investigate the influences of the incident light intensity and QE number density on the transmission response for this hybrid system.

The color-coded graphs for the influence of the incident intensity and QE number density on the pulse repetition frequency (PRF) and the extinction ratio [EXT = $10\log_{10}(T_{\max}/T_{\min}) = 10\log_{10}(a_{\max}/a_{\min})$] are shown in Figs. 4(a) and 4(b), respectively. To understand the mechanism of pulse formation more intuitively and deeply, the three points of $A(105, 0.8)$, $B(105, 1.2)$, and $C(170, 1.2)$ are chosen for comparison. First, we analyze the formation mechanism of the femtosecond pulse shown in Fig. 5(b). The phase in Eq. (14) can be expressed as $\varphi_{\mathrm{nw}}(t) = \int_0^t \Omega_R(t)\,dt$. The process from 0 to t_1 is called stage I. In stage I, $0 < \varphi_{\mathrm{nw}}(t) < \pi$, $p_{\mathrm{nw}} < 0$. This indicates that the nanowire is absorbing energy, so the extra field amplitude a_{nw} is negative, that is, $a_{\mathrm{nw}} < 0$. The total field amplitude in the resonator is $a = a_0 + a_{\mathrm{nw}} < a_0$. According to the transmittance expression [Eq. (26)] of the system, it can be obtained that $T < T_0$. The process from t_1 to t_2 is called stage II. In stage II, $\pi < \varphi_{\mathrm{nw}}(t) < 3\pi/2$, $p_{\mathrm{nw}} > 0$. This indicates that the nanowire is releasing energy, so the extra field amplitude a_{nw} is positive, that is, $a_{\mathrm{nw}} > 0$. The total field amplitude in the resonator is $a > a_0$, so $T > T_0$. According to Eq. (14), it can be known that the output power of the nanowire increases over time in stage II, resulting in the total field amplitude in the resonator increasing over time. According to Eq. (26), the transmittance of the system will also increase over time and reaches its maximum at t_2. The process from t_2 to t_3 is called stage III. Stage III is the time mirror of stage II.

In the whole process from 0 to t_3, the energy absorbed by the nanowire in stage I is released in stages II and III. All the energy in nanowire is completely released at t_3, and the
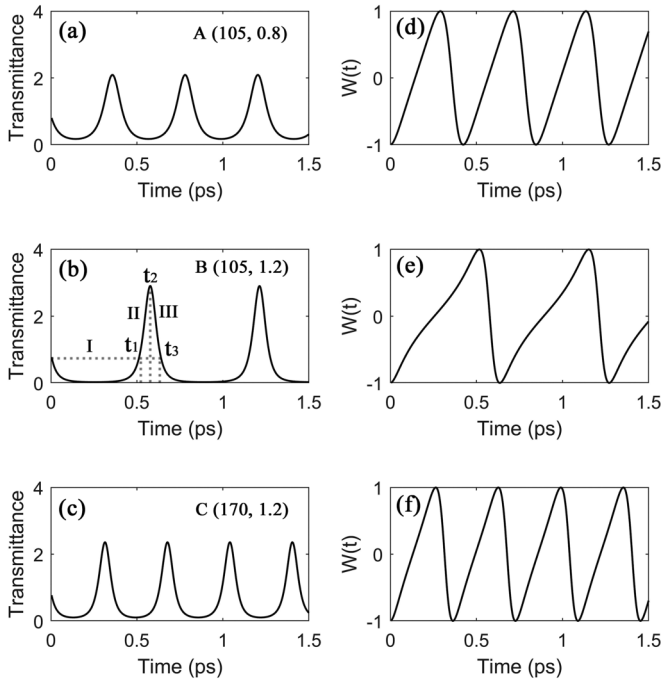
FIG. 5. (a)–(c) Curves for the transmittance changing over time at the three points A, B, and C. (d)–(f) Curves for the population difference function $W(t)$ changing over time at the three points A, B, and C, respectively.
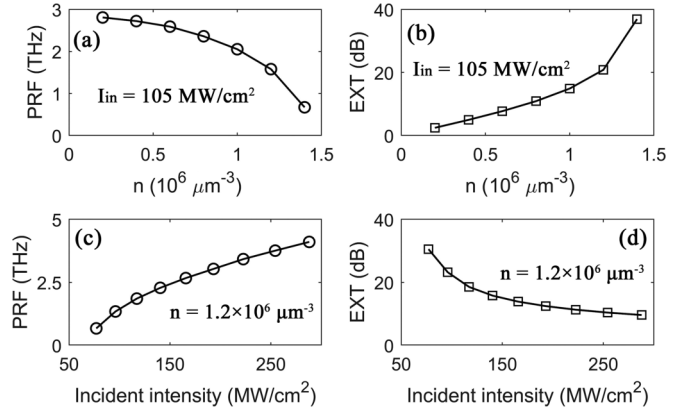

FIG. 6. Curves for (a) PRF and (b) EXT changing with the number density of QEs when the incident intensity is $I_{\text{in}} = 105$ MW/cm^2. Curves for (c) PRF and (d) EXT changing with the incident intensity when the number density of QEs is $n = 1.2 \times 10^6$ μm^{-3}.

system returns to the initial state. According to the analysis in the previous paragraph, the total field amplitude in stage I is smaller than that in stages II and III, so the rate of phase change $\varphi'_{\text{nw}}(t) = \Omega_R(t)$ in stage I is smaller than that in stages II and III. In this case, the duration of stage I is longer than the sum of the duration of stages II and III, that is, $t_1 > t_3 - t_1$. Therefore, the transmittance of the system will appear as pulse form. In Fig. 5(b), the pulse width is 83 fs, and the repetition frequency is 1.67 THz. This result indicates that it is feasible to generate femtosecond pulses with THz repetition frequencies in plasmonic resonator systems using a continuous wave input.

The calculated results show that the incident light intensity and the QE number density both have impacts on the pulse repetition frequency and the extinction ratio. The effect of QE number density on PRF and EXT can be understood by comparing Figs. 5(a) and 5(b). The incident intensity of point A and point B are the same, while the QE number density of point A is smaller than that of point B. According to Eq. (14), when the incident intensity is constant, the greater the QE number density, the larger the absorbed power density of the nanowire in stage I, then the smaller the total field amplitude, so the duration of stage I will be longer. But the QE number density has little effect on the duration of stages II and III. Therefore, the greater the QE number density, the longer the pulse period, then the smaller the PRF, as shown in Fig. 6(a). On the other hand, the greater the QE number density, the lager the total field amplitude at t_2. According to the definition of the extinction ratio, it can be known that the EXT of the system will be larger, as shown in Fig. 6(b). In Figs. 6(a) and 6(b), as the QE number density n increases from 0.2×10^6 to 1.4×10^6 μm^{-3}, the repetition frequency of the pulse decreases from 2.8 to 0.67

THz, whereas the extinction ratio increases from 2.4 to 37 dB. Conversely, when the QE number density approaches to 0, PRF and EXT approach to $\chi|a_0|$ and 0, respectively. Since $\Omega_R(t) = \chi|a(t)|$, Eq. (25) is not a linear equation but a complex nonlinear equation, resulting in the nonlinear dependence of PRF and EXT on the incident intensity and the QE number density.

The effect of the incident intensity on PRF and EXT can be understood by comparing Figs. 5(b) and 5(c). The QE number density of points B and C are the same, while the incident intensity of point B is smaller than that of point C. When the QE number density is constant, according to the calculation results based on Eq. (25), the greater the incident intensity, the larger the total field amplitude in the three stages. Therefore, the time required for the phase to change from 0 to 2π will be shorter, then the PRF will be larger, as shown in Fig. 6(c). And the greater the incident intensity, the smaller the influence of output power of the nanowire on the transmission power. So, the EXT will be smaller, as shown in Fig. 6(d). In Figs. 6(c) and 6(d), the repetition frequency of the pulses increases from 0.67 to 4.1 THz as the incident intensity increases from 77 to 288 MW/cm^2, but the extinction ratio decreases from 31 to 9.6 dB. And when the incident intensity is extremely large, the PRF and EXT approach $\chi|a_0|$ and 0, respectively. In addition, by comparing Figs. 5(d)–5(f), it can be found that the greater the ratio of the QE number density to the incident intensity, the closer the population difference function curve is to a zigzag of which the front slope is gentle and the back slope is steep, and the closer the transmittance curve is to comb-pulse form.

The plasmon-generated femtosecond pulses are also reported in other recent works. In the report of Sámson *et al.* [32], the pulse duration (broadening and narrowing) and intensity decay (acceleration and retardation) are controlled by the group velocity and loss dispersion effects. To be different from them, we use the incident light intensity and QE number density to control the pulse repetition frequency and extinction ratio. For the generation of femtosecond pulses in plasmonic systems, the two methods can complement each other. Moreover, Kim *et al.* predicted the possibility of SPP pulse generation with ∼100 fs pulse duration [33]. While our method not only achieves pulses

with widths below 100 fs, but also allows repetition frequencies to reach the order of THz.

Moreover, when the ratio of the QE number density to the incident intensity is too large (this means $n \to \infty$ or $I_{\text{in}} \to 0$), the semiclassical theoretical model presented in this paper is no longer applicable, and it needs to be discussed with full quantum theory. The related research will be carried out in our followup work.

V. CONCLUSION

In summary, we have investigated the transmission response of a hybrid system composed of a VG plasmonic resonator coupled to a nanowire embedded with two-level QEs. Femtosecond pulses with THz repetition frequency can be obtained by the coupling between the QEs and the plasmonic resonator in the case of continuous wave input. The repetition frequency and extinction ratio of the pulses can be freely controlled by the incident light intensity and QE number density. The pulse widths can be modulated below 100 fs, and the extinction ratio can also reach very high values. This provides a method for generating narrow pulsed lasers with ultrahigh repetition frequency in plasmonic resonator systems; it has potential applications for generating optical clock signals at the nanoscale.

ACKNOWLEDGMENTS

[1] N. P. de Leon, M. D. Lukin, and H. Park, Quantum plasmonic circuits, IEEE J. Sel. Top. Quantum Electron **18**, 1781 (2012).

[2] J. O'Brien, B. Patton, M. Sasaki, and J. Vučković, Focus on integrated quantum optics, New J. Phys. **15**, 035016 (2013).

[3] P. Törmä and W. L. Barnes, Strong coupling between surface plasmon polaritons and emitters, Rep. Prog. Phys. **78**, 013901 (2015).

[4] G. Romero, J. J. Garcia-Ripoll, and E. Solano, Microwave Photon Detector in Circuit QED, Phys. Rev. Lett. **102**, 173602 (2009).

[5] S. P. Burgos, H. W. Lee, E. Feigenbaum, R. M. Briggs, and H. A. Atwater, Synthesis and characterization of plasmonic resonant guided wave networks, Nano Lett. **14**, 3284 (2014).

[6] M. T. Hill and M. C. Gather, Advances in small lasers, Nat. Photon. **8**, 908 (2014).

[7] P. Berini and I. D. Leon, Surface plasmon-polariton amplifiers and lasers, Nat. Photon. **6**, 16 (2011).

[8] J. Zhang, J. Cai, Y. Bai, J. Gao, and S. Zhu, Optimization of the noise property of delayed light in electromagnetically induced transparency, Phys. Rev. A **76**, 033814 (2007).

[9] P. Vasa, W. Wang, R. Pomraenke, M. Lammers, M. Maiuri, C. Manzoni, G. Cerullo, and C. Lienau, Real-time observation of ultrafast Rabi oscillations between excitons and plasmons in metal nanostructures with J-aggregates, Nat. Photon. **7**, 128 (2013).

[10] A. Demetriadou, J. M. Hamm, Y. Luo, J. B. Pendry, J. J. Baumberg, and O. Hess, Spatio-temporal dynamics and control of strong coupling in plasmonic nano-cavities, ACS Photon. **4**, 2410 (2017).

[11] P. Molina, E. Yraola, M. O. Ramírez, C. Tserkezis, J. L. Plaza, J. Aizpurua, J. Bravo-Abad, and L. E. Bausá, Plasmon-assisted Nd3+-based solid-state nanolaser, Nano Lett. **16**, 895 (2016).

[12] M. S. Tame, K. R. McEnery, Ş. K. Özdemir, J. Lee, S. A. Maier, and M. S. Kim, Quantum plasmonics, Nat. Phys. **9**, 329 (2013).

[13] D. K. Gramotnev and S. I. Bozhevolnyi, Plasmonics beyond the diffraction limit, Nat. Photon. **4**, 83 (2010).

[14] W. L. Barnes, A. Dereux, and T. W. Ebbesen, Surface plasmon subwavelength optics, Nature (London) **424**, 824 (2003).

[15] J. Ren, Y. Gu, D. Zhao, F. Zhang, T. Zhang, and Q. Gong, Evanescent-Vacuum-Enhanced Photon-Exciton Coupling and Fluorescence Collection, Phys. Rev. Lett. **118**, 073604 (2017).

[16] D. E. Chang, A. S. Sørensen, P. R. Hemmer, and M. D. Lukin, Quantum Optics with Surface Plasmops, Phys. Rev. Lett. **97**, 053002 (2006).

[17] K. C. Y. Huang, M.-K. Seo, T. Sarmiento, Y. Huo, J. S. Harris, and M. L. Brongersma, Electrically driven subwavelength optical nanocircuits, Nat. Photon. **8**, 244 (2014).

[18] H. Wei and H. Xu, Nanowire-based plasmonic waveguides and devices for integrated nanophotonic circuits, Nanophotonics **1**, 155 (2012).

[19] A. D. Jameson, J. L. Tomaino, Y.-S. Lee, G. Khitrova, H. M. Gibbs, C. N. Böttge, A. C. Klettke, M. Kira, and S. W. Koch, Direct measurement of light matter energy exchange inside a microcavity, Optica **1**, 276 (2014).

[20] M. Ramezani, A. Halpin, A. I. Fernández-Domínguez, J. Feist, S. R.-K. Rodriguez, F. J. Garcia-Vidal, and J. Gómez Rivas, Plasmon-exciton-polariton lasing, Optica **4**, 31 (2017).

[21] D. F. P. Pile and D. K. Gramotnev, Channel plasmon-polariton in a triangular groove on a metal surface, Opt. Lett. **29**, 1069 (2004).

[22] D. F. P. Pile and D. K. Gramotnev, Plasmonic subwavelength waveguides: Next to zero losses at sharp bends, Opt. Lett. **30**, 1186 (2005).

[23] E. Moreno, F. J. Garcia-Vidal, S. G. Rodrigo, L. Martin-Moreno, and S. I. Bozhevolnyi, Channel plasmon-polaritons: Modal shape, dispersion, and losses, Opt. Lett. **31**, 3447 (2006).

[24] Z. Han and S. I. Bozhevolnyi, Radiation guiding with surface plasmon polaritons, Rep. Prog. Phys. **76**, 16402 (2013).

[25] V. J. Sorger, R. F. Oulton, R. M. Ma, and X. Zhang, Toward integrated plasmonic circuits, MRS Bull. **37**, 728 (2012).

[26] P. B. Johnson and R. W. Christy, Optical constants of the noble metals, Phys. Rev. B **6**, 4370 (1972).

[27] K. E. Oughstun and N. A. Cartwright, On the Lorentz-Lorenz formula and the Lorentz model of dielectric dispersion, Opt. Express **11**, 1541 (2003).

[28] S. Raza, N. Stenger, A. Pors, T. Holmgaard, S. Kadkhodazadeh, J. B. Wagner, K. Pedersen, M. Wubs, S. I. Bozhevolnyi, and

N. A. Mortensen, Extremely confined gap surface-plasmon modes excited by electrons, Nat. Commun. **5**, 4125 (2014).

[29] J. R. Ackerhalt and B. W. Shore, Rate equations versus Bloch equations in multiphoton ionization, Phys. Rev. A **16**, 277 (1977).

[30] S. Li, Y. Wang, R. Jiao, L. Wang, G. Duan, and L. Yu, Fano resonances based on multimode and degenerate mode interference in plasmonic resonator system, Opt. Express **25**, 3525 (2017).

[31] E. Waks and J. Vuckovic, Dipole Induced Transparency in Drop-Filter Cavity-Waveguide Systems, Phys. Rev. Lett. **96**, 153601 (2006).

[32] Z. L. Sámson, P. Horak, K. F. MacDonald, and N. I. Zheludev, Femtosecond surface plasmon pulse propagation, Opt. Lett. **36**, 250 (2011).

[33] K.-H. Kim, A. Husakou, and J. Herrmann, Theory of plasmonic femtosecond pulse generation by mode-locking of long-range surface plasmon polariton, Opt. Express **20**, 462 (2012).